Spin polarized enantio-sensitive multipolar photoelectron currents

Philip Caesar M. Flores,[1] Stefanos Carlström,[1] Serguei Patchkovskii,[1] Andres F. Ordonez,[2,3] and Olga Smirnova[1,4,5]

[1] *Max-Born-Institut, Max-Born-Str. 2A, 12489 Berlin, Germany*
[2] *Department of Physics, Imperial College London, SW7 2BW London, United Kingdom*
[3] *Department of Chemistry, Queen Mary University of London, E1 4NS London, United Kingdom*
[4] *Technische Universität Berlin, 10623 Berlin, Germany*
[5] *Technion, Haifa, Israel*

(Dated: May 12, 2025)

Photoelectron circular dichroism (PECD) manifests as a forward-backward asymmetry of electron emission in the direction orthogonal to the light polarization plane via one-photon ionization of chiral molecules with circularly polarized light. Multi-polar 'PECD' currents, i.e., currents resolved along multiple directions, have also been predicted using two mutually-orthogonal linearly polarized light with carrier frequencies ω and 2ω. These currents arise from the interference between the one- and two-photon transitions. Here, we will show that photoelectron spin detection reveals enantio-sensitive multi-polar currents already in the one-photon regime since the two axes can be marked by the photoelectron momentum $\hat{\boldsymbol{k}}$ and spin-detection axis $\hat{\boldsymbol{s}}$. Specifically, we consider one-photon ionization of an isotropic ensemble of randomly oriented chiral molecules via circularly polarized light and show that the resulting spin-resolved current has three components whose magnitudes are comparable and can be larger than PECD: (i) a spin-polarization vortex in the plane of light polarization that rotates in opposite directions for opposite enantiomers, (ii) either a spin-sink or source in the plane of light polarization for opposite enantiomers, and (iii) a spin analog of photoelectron vortex dichroism (Phys. Rev. Lett. **129**, 233201, 2022) wherein the detected photoelectron spin encodes molecular chirality.

Photoelectron circular dichroism (PECD) heralded the "dipole revolution" in chiral discrimination: chiral discrimination without using chiral light [1, 2]. It was first predicted by Ritchie [3] and first detected by Böwering *et. al.* [4]. Nowadays, PECD is very well established theoretically, and also shown to yield strong enantiosensitive signals across several molecular species [5–18]. In PECD, the photoionization of an isotropic ensemble of randomly oriented chiral molecules via circularly polarized light results to a forward-backward asymmetry in the net photoelectron current in the direction of light polarization. Fundamentally, it can be understood as a manifestation of a geometric magnetic field introduced in Ref. [1], and its emergence leads to new enantio-sensitive observables in photoionization [2, 19].

Geometric magnetism in photoionization [19] and photoexcitation [20] of chiral molecules addresses the dynamical origin of enantiosensitive observables in one or multiphoton ionization [1, 19]. Its central object – the geometric propensity field:

$$\vec{\boldsymbol{B}}^{M}_{\vec{\boldsymbol{k}}^M} \equiv i\vec{\boldsymbol{D}}^{M*}_{\vec{\boldsymbol{k}}^M} \times \vec{\boldsymbol{D}}^{M}_{\vec{\boldsymbol{k}}^M}, \tag{1}$$

– presents the spin of the photoelectron dipole field[1] and underlies several classes of such observables relying on: (i) the net propensity field $\vec{\boldsymbol{\Omega}} \equiv \int d\Theta_k \vec{\boldsymbol{B}}_{\vec{\boldsymbol{k}}}$; (ii) the net radial component of the propensity field $B^{\parallel} \equiv \int d\Theta_k (\hat{\boldsymbol{k}} \cdot \vec{\boldsymbol{B}}_{\vec{\boldsymbol{k}}})$; and (iii) the spherical multipole moments of the longitudinal and transversal field components $B^{\parallel}_{l,m} \equiv \int d\Theta_k (\hat{\boldsymbol{k}} \cdot \vec{\boldsymbol{B}}_{\vec{\boldsymbol{k}}}) Y_{l,m}$, $B^{\perp,1}_{l,m} \equiv \int d\Theta_k \vec{\boldsymbol{B}}_{\vec{\boldsymbol{k}}} \cdot \nabla_k Y_{l,m}$, and $B^{\perp,2}_{l,m} \equiv \int d\Theta_k \vec{\boldsymbol{B}}_{\vec{\boldsymbol{k}}} \cdot (\hat{\boldsymbol{k}} \times \nabla_k) Y_{l,m}$.

Photoelectron circular dichroism belongs to the Class II observables. The Class I observables have been explored in Ref. [19], where it was shown that the net propensity field $\vec{\boldsymbol{\Omega}}$ controls the enantio-sensitive orientation of the cations (MOCD - molecular orientation circular dichroism). The Class III observables have tensorial nature and represent multipolar photoelectron currents, i.e., currents resolved along multiple directions. These currents arise due to the longitudinal and transversal components of the propensity field. The properties of one of such observables emerging in two photon ionization by two-color fields due to interference between the one- and two-photon transitions have been explored theoretically in Refs. [21–23]. The same two-color set-up enabled detection of its possible analogue in multiphoton regime [24]. However, these effects ignore the photoelectron spin. Spin detection opens an exciting opportunity to reveal enantio-sensitive multipolar currents arising already in the one-photon regime. Indeed, the two axes needed to resolve such currents can be marked by the photoelectron momentum $\hat{\boldsymbol{k}}^L$ and spin-detection axis $\hat{\boldsymbol{s}}^L$.

The analysis of the interplay of chirality and spin in photoionization of chiral molecules was pioneered by Cherepkov [25–27]. He identified a *kinematic* picture of spin polarization, predicting spin-and enantio-sensitive effects in one photon ionization for circularly and lin-

[1] Superscripts L and M are used to denote quantities in the laboratory and molecular frames, respectively. Vectors in the molecular frame, $\vec{\boldsymbol{a}}^M$, are transformed into the laboratory frame using the relation $\vec{\boldsymbol{a}}^L = R_\rho \vec{\boldsymbol{a}}^M$, where R_ρ is the Euler rotation matrix.

early polarized light. First experiments detecting spin polarization in multiphoton ionization have just appeared [28]; simulations predicting spin-polarization in PECD have also become possible [29]. We have also recently identified [30] a spin-resolved variant of geometric magnetism arising in chiral molecules, leading to a new effect: enantio-sensitive locking of the molecular cation orientation to the photoelectron spin. Here we use our formalism [30] to explore the Class III observables. We show how the spin-resolved propensity field generates spin-polarized enantio-sensitive multi-polar currents in one-photon ionization. Our results, which are consistent with predictions by Cherepkov [25–27], allow us to identify the physical mechanisms underlying these effects. We also demonstrate that spin-polarised enantio-sensitive currents are comparable and can exceed PECD.

We start by introducing spin-resolved propensity field:

$$\vec{\boldsymbol{B}}^{L}_{\vec{\boldsymbol{k}}^M,\mu^M} \equiv i\vec{\boldsymbol{D}}^{L*}_{\vec{\boldsymbol{k}}^M,\mu^M} \times \vec{\boldsymbol{D}}^{L}_{\vec{\boldsymbol{k}}^M,\mu^M}, \tag{2}$$

where $\vec{\boldsymbol{D}}^{L}_{\vec{\boldsymbol{k}}^M,\mu^M}$ is the spin-resolved photoionization dipole

$$\vec{\boldsymbol{D}}^{L}_{\vec{\boldsymbol{k}}^M,\mu^M} \equiv \langle \psi_f; \varphi^{(-)}_{\vec{\boldsymbol{k}}^M,\mu^M} | \vec{\boldsymbol{d}}^{L} | \psi_i \rangle. \tag{3}$$

The spin-resolved continuum state with momentum $\vec{\boldsymbol{k}}^M$ is denoted by $\varphi^{(-)}_{\vec{\boldsymbol{k}}^M,\mu^M}$, $|\psi_f\rangle$ is a final state of the ion, and $\mu^M = \pm\frac{1}{2}$ is the spin projection on the z-axis of the the molecular frame $\hat{\boldsymbol{\zeta}}^M$. For opposite enantiomers, the transition dipoles are related as $\vec{\boldsymbol{D}}^{L(R)}_{\vec{\boldsymbol{k}}^M,\mu^M} = -\vec{\boldsymbol{D}}^{L(S)}_{-\vec{\boldsymbol{k}}^M,\mu^M}$ [31]. It is also instructive to introduce the spin-symmetric and antisymmetric propensity fields,

$$\vec{\boldsymbol{B}}^{L}_{\vec{\boldsymbol{k}}^M,\pm} \equiv \frac{1}{2}\left(\vec{\boldsymbol{B}}^{L}_{\vec{\boldsymbol{k}}^M,\frac{1}{2}} \pm \vec{\boldsymbol{B}}^{L}_{\vec{\boldsymbol{k}}^M,-\frac{1}{2}}\right). \tag{4}$$

The spin-symmetric field $\vec{\boldsymbol{B}}^{L}_{\vec{\boldsymbol{k}}^M,+}$ is not sensitive to spin and has similar properties to $\vec{\boldsymbol{B}}^{L}_{\vec{\boldsymbol{k}}^M}$ in Eq. (1), emerging without spin-orbit interaction [19]. The spin-antisymmetric field $\vec{\boldsymbol{B}}^{L}_{\vec{\boldsymbol{k}}^M,-}$ arises only in the presence of spin-orbit interaction and underlies the appearance of spin-polarized enantio-sensitive observables.

Consider one-photon ionization by circularly polarized light $\vec{\boldsymbol{E}}^{L} = E^{L}_{\omega}(\hat{\boldsymbol{x}}^{L} + i\xi\hat{\boldsymbol{y}}^{L})/\sqrt{2}$ from the ground state of a molecule. Here ω is the photon energy and $\xi = \pm 1$ characterizes the direction of rotation of the light polarization vector. The momentum and spin resolved photoionization rate of a randomly oriented ensemble of molecules is

$$W^{L}(\hat{\boldsymbol{k}}^{L}, \hat{\boldsymbol{s}}^{L}) = \int d\rho W^{M}(\hat{\boldsymbol{k}}^{M}, \hat{\boldsymbol{s}}^{L}, \rho), \tag{5a}$$

$$= \sum A^{\ell,m_\ell}_{\ell_s,m_s} Y_{\ell,m_\ell}(\hat{\boldsymbol{k}}^{M}) Y_{\ell_s,m_s}(\hat{\boldsymbol{s}}^{L}) \tag{5b}$$

where the orientation $\rho \equiv \alpha\beta\gamma$ is defined by the Euler angles, $\int d\rho \equiv \frac{1}{8\pi^2}\int_0^{2\pi} d\alpha \int_0^{\pi} d\beta \sin\beta \int_0^{2\pi} d\gamma$, and $W^{M}(\hat{\boldsymbol{k}}^{M}, \hat{\boldsymbol{s}}^{L}, \rho)$ is the photoionization rate in the molecular frame for a given orientation ρ with the photoelectron spin measured along $\hat{\boldsymbol{s}}^{L}$ [30]:

$$W^{M}(\hat{\boldsymbol{k}}^{M}, \hat{\boldsymbol{s}}^{L}, \rho) = \frac{1}{2}\sum_{\mu^M} \left|\vec{\boldsymbol{D}}^{L}_{\vec{\boldsymbol{k}}^M,\mu^M} \cdot \vec{\boldsymbol{E}}^{L}\right|^2 \left(1 + \hat{\boldsymbol{s}}^{L} \cdot \hat{\boldsymbol{\sigma}}^{L}_{\mu^M,\mu^M}\right). \tag{6}$$

Here, $\hat{\mathsf{P}}_{\hat{\boldsymbol{s}}^L} = \left(\mathbb{I} + \hat{\boldsymbol{s}}^{L} \cdot \hat{\boldsymbol{\sigma}}^{L}\right)/2$ is a spin projection operator with respect to $\hat{\boldsymbol{s}}^{L}$, $\hat{\boldsymbol{\sigma}}^{L}$ is the vector of Pauli spin matrices, and $\hat{\boldsymbol{\sigma}}^{L}_{\mu^M,\mu^M} \equiv \langle \chi_{\mu^M} | \hat{\boldsymbol{\sigma}}^{L} | \chi_{\mu^M} \rangle$ is spin quantization axis. Essentially, the spin-projection operator $\hat{\mathsf{P}}_{\hat{\boldsymbol{s}}^L}$ rotates the photoelectron spin quantization axis (z-axis of the molecular frame $\hat{\boldsymbol{\zeta}}^{M}$), to $\hat{\boldsymbol{\zeta}}^{L} = R_\rho \hat{\boldsymbol{\zeta}}^{M}$, then projects it to $\hat{\boldsymbol{s}}^{L}$ where it is measured.

Eqs. (5a) and (6) show that integrating the $\hat{\boldsymbol{s}}^{L}$-independent terms yields the usual momentum-resolved photoionization yield, from which the PECD current, which is proportional to $A^{1,0}_{0,0}$, can be extracted directly:

$$\begin{aligned}\vec{\boldsymbol{j}}^{L}_{\mathrm{PECD}} &= \frac{1}{2}\sum_{\mu^M}\int d\Theta^{M}_{k}\int d\rho \left|\vec{\boldsymbol{D}}^{L}_{\vec{\boldsymbol{k}}^M,\mu^M} \cdot \vec{\boldsymbol{E}}^{L}\right|^2 \vec{\boldsymbol{k}}^{M} \\ &= \left[\frac{1}{6}\int d\Theta^{M}_{k}\left(\vec{\boldsymbol{k}}^{M} \cdot \vec{\boldsymbol{B}}^{M}_{\vec{\boldsymbol{k}}^M,+}\right)\right]\vec{\boldsymbol{\Xi}}^{L} \\ &= \left[\frac{1}{6k}\int d\vec{\boldsymbol{\Theta}}^{M} \cdot \vec{\boldsymbol{B}}^{M}_{\vec{\boldsymbol{k}}^M,+}\right]\vec{\boldsymbol{\Xi}}^{L}.\end{aligned} \tag{7}$$

Here $\int d\Theta^{M}_{k}$ denotes integration over all photoelectron directions; $\vec{\boldsymbol{\Xi}}^{L} = -i(\vec{\boldsymbol{E}}^{L*} \times \vec{\boldsymbol{E}}^{L}) = \xi|E^{L}_{\omega}|^2 \hat{\boldsymbol{z}}^{L}$ is the direction of photon spin. Eq.(7) is equal to the PECD current we derived in [32], to the original expression derived by Ritchie [3], without spin, and to the coefficient D introduced by Cherepkov [25–27]. Eq. (7) shows that the PECD current is not spin sensitive and is given by the flux of the spin-symmetric propensity field through the surface of the energy shell ($d\vec{\boldsymbol{\Theta}}^{M} = d\Theta^{M}_{k}\hat{\boldsymbol{k}}^{M}k^2$).

Similarly, the spin-resolved enantio-sensitive current conditioned on the photoelectron spin measured parallel to the $\hat{\boldsymbol{s}}^{L}$ axis is

$$\begin{aligned}\vec{\boldsymbol{j}}^{L}_{\hat{\boldsymbol{s}}} &= \frac{1}{2}\sum_{\mu^M}\int d\Theta^{M}_{k} \\ &\quad \times \int d\rho \left|\vec{\boldsymbol{D}}^{L}_{\vec{\boldsymbol{k}}^M,\mu^M} \cdot \vec{\boldsymbol{E}}^{L}\right|^2 \left(\hat{\boldsymbol{s}}^{L} \cdot \hat{\boldsymbol{\sigma}}^{L}_{\mu^M,\mu^M}\right)\vec{\boldsymbol{k}}^{M} \\ &= \vec{\boldsymbol{j}}^{L}_{\times} + \vec{\boldsymbol{j}}^{L}_{\parallel} + \vec{\boldsymbol{j}}^{L}_{\perp}\end{aligned} \tag{8a}$$

The three components of $\vec{\boldsymbol{j}}^{L}_{\hat{\boldsymbol{s}}}$ are illustrated in Fig. 1 which we discuss below.

The current $\vec{\boldsymbol{j}}^{L}_{\times}$ arises from the 'coupling' of the photoelectron spin quantization axis $\hat{\boldsymbol{\sigma}}^{M}_{\frac{1}{2},\frac{1}{2}}$ to the transverse component of the spin-antisymmetric propensity field $\vec{\boldsymbol{B}}^{M}_{\vec{\boldsymbol{k}}^M,-} \times \vec{\boldsymbol{k}}^{M}$:

$$\vec{\boldsymbol{j}}^{L}_{\times} = \left\{\frac{1}{12}\int d\Theta^{M}_{k}\left[\hat{\boldsymbol{\sigma}}^{M}_{\frac{1}{2},\frac{1}{2}} \cdot \left(\vec{\boldsymbol{B}}^{M}_{\vec{\boldsymbol{k}}^M,-} \times \vec{\boldsymbol{k}}^{M}\right)\right]\right\}\left(\hat{\boldsymbol{s}}^{L} \times \vec{\boldsymbol{\Xi}}^{L}\right) \tag{9}$$

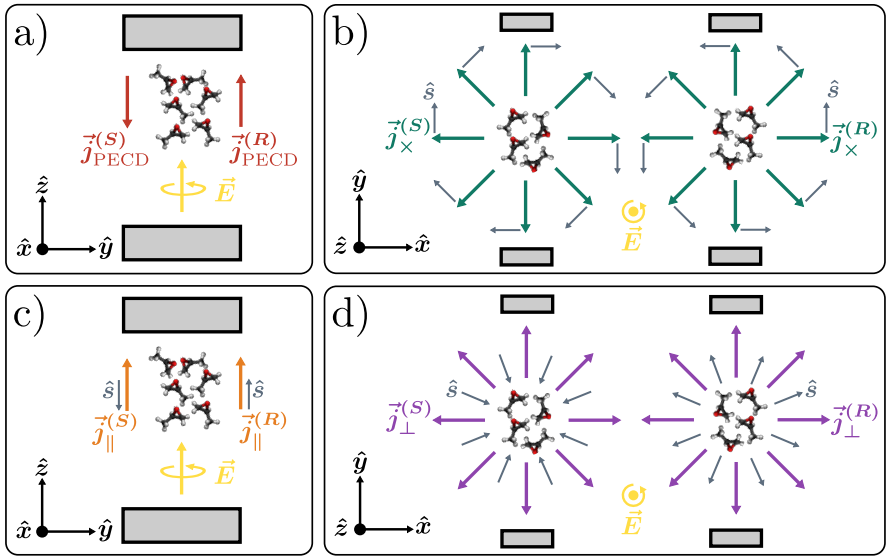

FIG. 1. Schematic view of the (a) PECD current $\vec{\jmath}^{L}_{\mathrm{PECD}}$ compared with the (b-d) three components of the spin-resolved current $\vec{\jmath}^{L}_{\hat{\boldsymbol{s}}}$. The superscripts (S) and (R) denotes the corresponding current for the left and right-handed enantiomer.

Since the direction of the current $\vec{\jmath}^{L}_{\times}$ in the laboratory frame is defined by the cross product of the photon spin vector $\vec{\Xi}^{L}$ and photoelectron spin detection axis $\hat{\boldsymbol{s}}^{L}$, then $\vec{\jmath}^{L}_{\times}$ is confined to the polarization plane and spin-polarization is transversal. This current is equivalent to the coefficient C of Cherepkov [25–27], in which $\vec{\jmath}^{L}_{\times} \propto A^{1,1}_{1,-1} - A^{1,-1}_{1,1}$. The enantio-sensitive nature of $\vec{\jmath}^{L}_{\times}$ arises from the molecular factor $\hat{\boldsymbol{\sigma}}^{M}_{\frac{1}{2},\frac{1}{2}} \cdot (\vec{\boldsymbol{B}}^{M}_{\vec{\boldsymbol{k}}^{M},-} \times \vec{\boldsymbol{k}}^{M})$ which is a pseudoscalar: opposite enantiomers produce opposite spin vortices, such that spin polarization direction depends on photoelectron momentum in a way reminiscent of Rashba effect in solids.

Now, the molecular factor of $\vec{\jmath}^{L}_{\times}$ can equivalently be expressed as

$$\begin{aligned} B^{\perp,2}_{1,0} &= \int d\Theta^{M}_{k} \left[\hat{\boldsymbol{\sigma}}^{M}_{\frac{1}{2},\frac{1}{2}} \cdot \left(\vec{\boldsymbol{B}}^{M}_{\vec{\boldsymbol{k}}^{M},-} \times \vec{\boldsymbol{k}}^{M}\right)\right] \\ &= \int d\Theta^{M}_{k} \left[\vec{\boldsymbol{B}}^{M}_{\vec{\boldsymbol{k}}^{M},-} \cdot (\vec{\boldsymbol{k}}^{M} \times \nabla) Y_{1,0}(\vec{\boldsymbol{k}}^{M})\right] \end{aligned} \tag{10}$$

which indicates that $\vec{\jmath}^{L}_{\times}$ belongs to the Class III enantio-sensitive observables. Thus, to find spin-sensitive effects, we have to consider multipolar photoelectron currents, i.e. currents resolved along two orthogonal directions. Without spin detection, multipolar enantio-sensitive currents could be induced using orthogonally polarised two-color fields [2, 21, 23, 24], and recorded via interference between the two photoionization pathways involving the interference of one-photon and two-photon transitions. Spin detection opens an exciting opportunity to detect enantio-sensitive multipolar currents already in the one-photon regime, because the orthogonal axes can be marked by the photoelectron momentum and its spin. Since spin is a pseudovector, such detection scheme reveals the tensorial enantio-sensitive observables related to the tangential component of the propensity field – a new member of the Class III observables.

The currents $\vec{\jmath}^{L}_{\parallel}$ and $\vec{\jmath}^{L}_{\perp}$ do not arise from the propensity field, but rather from the helicity of the photoelectron $(\vec{\boldsymbol{k}}^{M} \cdot \hat{\boldsymbol{\sigma}}^{M}_{\frac{1}{2},\frac{1}{2}})$:

$$\begin{aligned} \vec{\jmath}^{L}_{\parallel} = &\left\{\frac{1}{15}\int d\Theta^{M}_{k} \mathcal{W}^{(2)}_{\vec{\boldsymbol{k}}} \left(\vec{\boldsymbol{k}}^{M} \cdot \hat{\boldsymbol{\sigma}}^{M}_{\frac{1}{2},\frac{1}{2}}\right)\right\} \\ &\left\{|\vec{\boldsymbol{E}}^{L}|^{2} (\hat{\boldsymbol{s}}^{L} \cdot \hat{\boldsymbol{z}}^{L}) \hat{\boldsymbol{z}}^{L}\right\} \end{aligned} \tag{11}$$

$$\begin{aligned} \vec{\jmath}^{L}_{\perp} = &\left\{\frac{1}{20}\int d\Theta^{M}_{k} \mathcal{W}^{(-3)}_{\vec{\boldsymbol{k}}} \left(\vec{\boldsymbol{k}}^{M} \cdot \hat{\boldsymbol{\sigma}}^{M}_{\frac{1}{2},\frac{1}{2}}\right)\right\} \\ &\left\{|\vec{\boldsymbol{E}}^{L}|^{2} \left[(\hat{\boldsymbol{s}}^{L} \cdot \hat{\boldsymbol{x}}^{L}) \hat{\boldsymbol{x}}^{L} + (\hat{\boldsymbol{s}}^{L} \cdot \hat{\boldsymbol{y}}^{L}) \hat{\boldsymbol{y}}^{L}\right]\right\}, \end{aligned} \tag{12}$$

which is weighted by the difference of the yields for the spin-up and spin-down photoelectrons

$$\mathcal{W}^{(\Lambda)}_{\vec{\boldsymbol{k}}} = R^{(\Lambda)}_{\frac{1}{2}} \left|\vec{\boldsymbol{D}}_{\vec{\boldsymbol{k}},\frac{1}{2}}\right|^{2} - R^{(\Lambda)}_{-\frac{1}{2}} \left|\vec{\boldsymbol{D}}_{\vec{\boldsymbol{k}},-\frac{1}{2}}\right|^{2}. \tag{13}$$

The quantity $R^{(\Lambda)}_{\vec{\boldsymbol{V}},\mu}$ accounts for how the geometry of the photoelectron dipole affects the yield:

$$R^{(\Lambda)}_{\mu} = 1 - \frac{1}{\Lambda} \frac{\mathrm{Re}\left[(\vec{\boldsymbol{D}}_{\vec{\boldsymbol{k}},\mu} \cdot \vec{\boldsymbol{k}}^{M})(\vec{\boldsymbol{D}}^{*}_{\vec{\boldsymbol{k}},\mu} \cdot \hat{\boldsymbol{\sigma}}_{\frac{1}{2},\frac{1}{2}})\right]}{|\vec{\boldsymbol{D}}_{\vec{\boldsymbol{k}},\mu}|^{2} (\vec{\boldsymbol{k}}^{M} \cdot \hat{\boldsymbol{\sigma}}^{M}_{\frac{1}{2},\frac{1}{2}})} \tag{14}$$

These currents present a spin polarization direction for opposite enantiomers that is (i) either parallel or anti-parallel to $\vec{\jmath}^{L}_{\parallel}$, and (ii) either forms a 'spin-sink' or

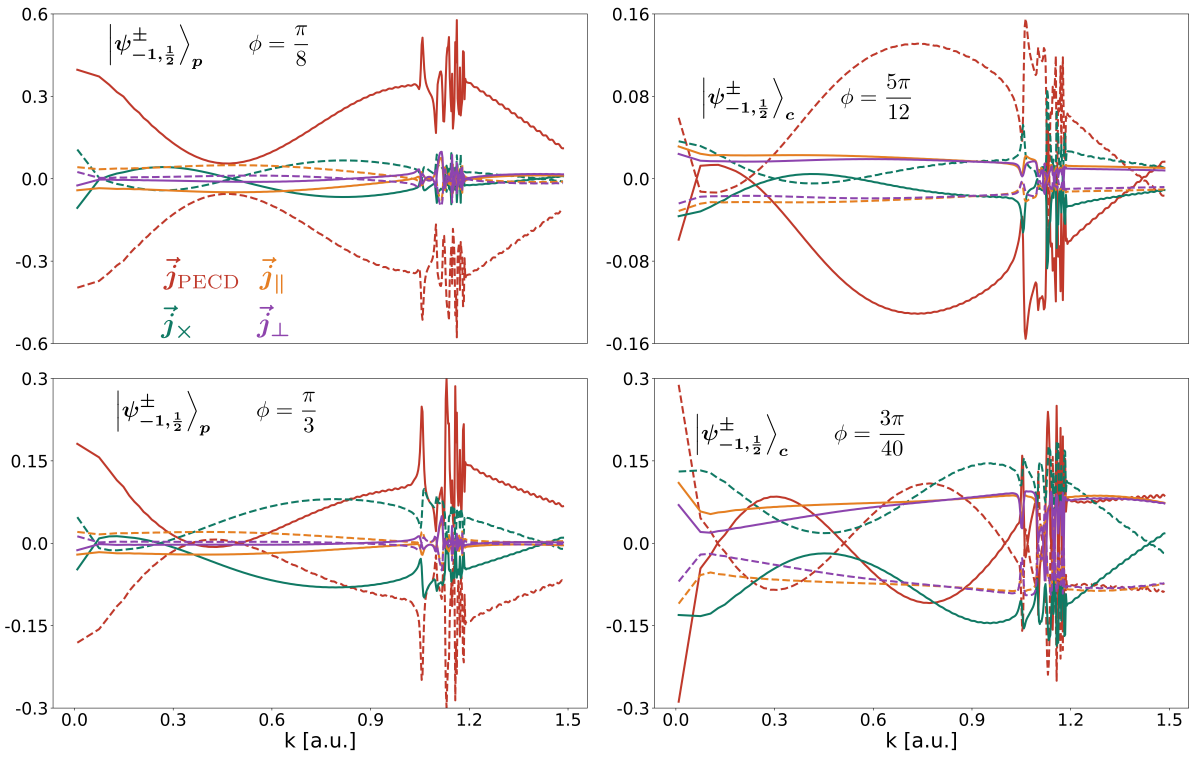

FIG. 2. Comparison of the currents for the chiral states $|\psi^{\pm}_{-1,\frac{1}{2}}\rangle_p$, and $|\psi^{\pm}_{-1,\frac{1}{2}}\rangle_c$. The solid and dashed lines represent the states $|\psi^{+}_{-1,\frac{1}{2}}\rangle_{p/c}$ and $|\psi^{-}_{-1,\frac{1}{2}}\rangle_{p/c}$, respectively. Red curve shows the PECD current, while yellow, green and violet show the three spin-sensitive and enantio-sensitive currents. The rapidly oscillating behavior at higher values of k is due to the Fano resonances, leading up to the ionization threshold for the 3s electrons [33, 34].

'spin-source' relative to $\vec{\boldsymbol{j}}^L_{\perp}$. Moreover, these currents also coincide with the coefficients B_1 and B_2 introduced by Cherepkov [25–27], in which $\vec{\boldsymbol{j}}^L_{\parallel} \propto A^{1,0}_{1,0} \propto B_2$ and $\vec{\boldsymbol{j}}^L_{\perp} \propto A^{1,1}_{1,-1} + A^{1,-1}_{1,1} \propto B_1$ [31].

Since both $\vec{\boldsymbol{j}} \parallel^L$ and $\vec{\boldsymbol{j}} \perp^L$ are independent of the photon spin direction, they can be driven by linearly polarised pulses. Of particular interest is the current $\vec{\boldsymbol{j}}^L_{\parallel}$, which serves as the spin analog of photoelectron vortex dichroism (PEVD) [35]. Specifically, PEVD uses linearly polarized light to generate photoelectrons with orbital angular momentum (OAM) wherein the OAM has opposite signs for opposite enantiomers, while $\vec{\boldsymbol{j}}^L_{\parallel}$ now suggests that photoelectrons with opposite spins are correlated to opposite enantiomers.

To quantify the effects, we will use the chiral state from our previous work [30], where both electronic chirality and spin-orbit coupling are accurately accounted for. It describes chiral electronic densities in an Ar atom excited into a chiral superposition of states

$$|\psi^{\pm}_{m,\mu}\rangle_p = (\cos\phi)|4p_m,\mu\rangle \pm (\sin\phi)|4d_m,\mu\rangle \tag{15}$$

$$|\psi^{\pm}_{m,\mu}\rangle_c = (\cos\phi)|4p_m,\mu\rangle \pm i(\sin\phi)|4d_m,\mu\rangle. \tag{16}$$

The eigenstates and associated spin-resolved photoionization dipole matrix elements of Ar atom were calculated using an atomic configuration-interaction singles treatment [34, 36, 37]. These states are inspired by a spinless chiral superposition in the hydrogen atom [1].

Figure 2 compares spin-resolved currents with PECD for various chiral superpositions with $m = -1$ and $\mu = \frac{1}{2}$. The currents are normalized to the total yield,

$$N = \int d\Theta^L_s \int d\Theta^M_k \int d\rho W^M(\hat{\boldsymbol{k}}^M, \hat{\boldsymbol{s}}^L, \rho) = \\ = \frac{1}{6}\left(\sum_{\mu^M} \int d\Theta^M_k \left|\vec{\boldsymbol{D}}^M_{\vec{\boldsymbol{k}}^M,\mu^M}\right|^2\right)|\vec{\boldsymbol{E}}^L|^2. \tag{17}$$

The PECD current $\vec{\boldsymbol{j}}_{\rm PECD}$ consistently yields strong enantio-sensitive signal as expected. The spin-resolved currents are more sensitive to the initial state, but can exceed the PECD current in some cases (bottom panels).

In conclusion, we have shown how measurements of the photo-electron spin can be used to detect a new Class III chiral observable – an enantio-sensitive spin vortex. We have identified the interplay of geometric and dynamical mechanisms underlying the emergence of these vortices in one-photon ionization of chiral molecules. We have also shown that these spin vortices can be as strong as spin-independent PECD currents.

We acknowledge discussions with Prof. M. Ivanov. O.S., A. O. and P.C.F. acknowledge ERC-2021-AdG project ULISSES, grant agreement No 101054696. A.O. acknowledges funding from the Royal Society URF/R1/201333, URF/ERE/210358, and URF/ERE/231177.

[1] A. F. Ordonez and O. Smirnova, Physical Review A **99**, 043416 (2019).
[2] D. Ayuso, A. F. Ordonez, and O. Smirnova, Physical Chemistry Chemical Physics **24**, 26962 (2022).
[3] B. Ritchie, Physical Review A **13**, 1411 (1976).
[4] N. Böwering, T. Lischke, B. Schmidtke, N. Müller, T. Khalil, and U. Heinzmann, Physical review letters **86**, 1187 (2001).
[5] I. Powis, The Journal of Chemical Physics **112**, 301 (2000).
[6] G. A. Garcia, L. Nahon, M. Lebech, J.-C. Houver, D. Dowek, and I. Powis, The Journal of chemical physics **119**, 8781 (2003).
[7] S. Turchini, N. Zema, G. Contini, G. Alberti, M. Alagia, S. Stranges, G. Fronzoni, M. Stener, P. Decleva, and T. Prosperi, Physical Review A—Atomic, Molecular, and Optical Physics **70**, 014502 (2004).
[8] U. Hergenhahn, E. E. Rennie, O. Kugeler, S. Marburger, T. Lischke, I. Powis, and G. Garcia, The Journal of chemical physics **120**, 4553 (2004).
[9] L. Nahon, G. A. Garcia, C. J. Harding, E. Mikajlo, and I. Powis, The Journal of chemical physics **125** (2006).
[10] G. A. Garcia, L. Nahon, C. J. Harding, and I. Powis, Physical Chemistry Chemical Physics **10**, 1628 (2008).
[11] M. H. Janssen and I. Powis, Physical Chemistry Chemical Physics **16**, 856 (2014).
[12] M. H. Janssen and I. Powis, Physical Chemistry Chemical Physics **16**, 856 (2014).
[13] L. Nahon, G. A. Garcia, and I. Powis, Journal of Electron Spectroscopy and Related Phenomena **204**, 322 (2015).
[14] C. Sparling and D. Townsend, Physical Chemistry Chemical Physics (2025).
[15] N. Cherepkov, Chemical Physics Letters **87**, 344 (1982).
[16] I. Powis, The Journal of Physical Chemistry A **104**, 878 (2000).
[17] M. Stener, G. Fronzoni, D. D. Tommaso, and P. Decleva, The Journal of chemical physics **120**, 3284 (2004).
[18] A. N. Artemyev, A. D. Müller, D. Hochstuhl, and P. V. Demekhin, The Journal of chemical physics **142** (2015).
[19] A. F. Ordonez, D. Ayuso, P. Decleva, and O. Smirnova, Communications Physics **6**, 257 (2023).
[20] A. F. Ordonez, A. Roos, P. M. Maier, D. Ayuso, and O. Smirnova, arXiv preprint arXiv:2409.02500 (2024).
[21] P. V. Demekhin, A. N. Artemyev, A. Kastner, and T. Baumert, Phys. Rev. Lett. **121**, 253201 (2018).
[22] P. V. Demekhin, Physical Review A **99**, 063406 (2019).
[23] A. F. Ordonez and O. Smirnova, Physical Chemistry Chemical Physics **24**, 7264 (2022).
[24] S. Rozen, A. Comby, E. Bloch, S. Beauvarlet, D. Descamps, B. Fabre, S. Petit, V. Blanchet, B. Pons, N. Dudovich, and Y. Mairesse, Phys. Rev. X **9**, 031004 (2019).
[25] N. Cherepkov, Journal of Physics B: Atomic and Molecular Physics **12**, 1279 (1979).
[26] N. Cherepkov, Journal of Physics B: Atomic and Molecular Physics **14**, 2165 (1981).
[27] N. Cherepkov, Journal of Physics B: Atomic and Molecular Physics **16**, 1543 (1983).
[28] A. Artemyev, R. Tomar, D. Trabert, D. Kargin, E. Kutscher, M. Schöffler, L. P. H. Schmidt, R. Pietschnig, T. Jahnke, M. Kunitski, *et al.*, Physical Review Letters **132**, 123202 (2024).
[29] A. N. Artemyev, E. Kutscher, B. M. Lagutin, and P. V. Demekhin, The Journal of Chemical Physics **158** (2023).
[30] P. C. M. Flores, S. Carlström, S. Patchkovskii, A. F. Ordonez, and O. Smirnova, arXiv preprint arXiv:2505.22433 (2024).
[31] P. C. M. Flores, S. Carlström, S. Patchkovskii, A. F. Ordonez, and O. Smirnova, In prepration (2024).
[32] A. F. Ordonez and O. Smirnova, Physical Review A **98**, 063428 (2018).
[33] J. Samson and W. Stolte, Journal of Electron Spectroscopy and Related Phenomena **123**, 265 (2002).
[34] S. Carlström, R. Tahouri, A. Papoulia, J. M. Dahlström, M. Y. Ivanov, O. Smirnova, and S. Patchkovskii, arXiv:2306.15665 [physics.atom-ph] (2024), manuscript submitted for review.
[35] X. B. Planas, A. Ordóñez, M. Lewenstein, and A. S. Maxwell, Physical Review Letters **129**, 233201 (2022).
[36] S. Carlström, M. Spanner, and S. Patchkovskii, Physical Review A **106**, 043104 (2022).
[37] S. Carlström, M. Bertolino, J. M. Dahlström, and S. Patchkovskii, Physical Review A **106**, 042806 (2022).